Food Chemistry: X 17 (2023) 100541

Contents lists available at ScienceDirect

Food Chemistry: X

journal homepage: www.sciencedirect.com/journal/food-chemistry-x

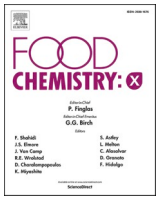

Non-destructive prediction of yak meat freshness indicator by hyperspectral techniques in the oxidation process

Kai Dong [a,b,1], Yufang Guan [c,1], Qia Wang [a,b], Yonghui Huang [c], Fengping An [b], Qibing Zeng [a,*], Zhang Luo [d,*], Qun Huang [a,b,e,f,*]

[a] The Key Laboratory of Environmental Pollution Monitoring and Disease Control, Ministry of Education, School of Public Health, Guizhou Medical University, Guiyang 550025, China
[b] Engineering Research Centre of Fujian-Taiwan Special Marine Food Processing and Nutrition of Ministry of Education, College of Food Science, Fujian Agriculture and Forestry University, Fuzhou, Fujian 350002, China
[c] The Food Processing Research Institute of Guizhou Province, Guizhou Academy of Agricultural Sciences/Potato Engineering Research Center of Guizhou Province/ Guizhou Key Laboratory of Agricultural Biotechnology, Guiyang 550006, Guizhou, China
[d] College of Food Science, Tibet Agriculture and Animal Husbandry University, Linzhi, Tibet Autonomous Region 860000, China
[e] Institute for Egg Science and Technology, School of Food and Biological Engineering, Chengdu University, Chengdu 610106, China
[f] Key Laboratory of Endemic and Ethnic Diseases, Ministry of Education & Key Laboratory of Medical Molecular Biology of Guizhou Province, Guizhou Medical University, Guiyang 550004, Guizhou, China

ARTICLE INFO

Keywords:
Hyperspectral technique
Yak meat
Freshness
PCR
SVR
PLSR

ABSTRACT

This study examined the potential of hyperspectral techniques for the rapid detection of characteristic indicators of yak meat freshness during the oxidation of yak meat. TVB-N values were determined by significance analysis as the characteristic index of yak meat freshness. Reflectance spectral information of yak meat samples (400–1000 nm) was collected by hyperspectral technology. The raw spectral information was processed by 5 methods and then principal component regression (PCR), support vector machine regression (SVR) and partial least squares regression (PLSR) were used to build regression models. The results indicated that the full-wavelength based on PCR, SVR, and PLSR models were shown greater performance in the prediction of TVB-N content. In order to improve the computational efficiency of the model, 9 and 11 characteristic wavelengths were selected from 128 wavelengths by successive projection algorithm (SPA) and competitive adaptive reweighted sampling (CARS), respectively. The CARS-PLSR model exhibited excellent predictive power and model stability.

1. Introduction

Yak meat has high protein content of 20 %–23 %, rich amino acids content and similar in structural ratio to the human body, which makes it an ideal meat product for people to choose. The unsaturated fatty acid content in yak meat is as high as 50 %–55 % (Huang et al., 2022). The instability of fat structure makes it easy to oxidize, and the free radicals generated by its oxidation will promote protein oxidation and destroy the amino acids in yak meat, which will lead to the loss of nutritional value and deterioration of yak meat quality. Therefore, the quality and safety of meat has been widely concerned (Wang et al., 2021).

Monitoring the freshness of yak meat during processing, storage and transportation to ensure food safety has become a hot issue. There are three general traditional methods for determining the freshness of yak meat: sensory assessment (Liu et al., 2020), microbiological assessment (Casaburi et al., 2015) and physical and chemical index test (Baek et al., 2021), but all of them are time-consuming and involve a large amount of experiments. To solve these problems, researchers tried their best to find some simple, quick, easy and less laborious methods to assess the freshness of meat.

In the last ten years or so, hyperspectral techniques, as a new type of rapid nondestructive testing method, have attracted much attention because of their advantages of high analytical efficiency, no need to break the sample, no complicated pre-treatment, and simultaneous analysis of multiple indicators (Yang, Sun, & Cheng, 2017). Hyperspectral technology has been widely used in the detection and

* Corresponding authors at: Guizhou Medical University, Gui 'an New District, Guizhou Province 550025, China.
E-mail addresses: 178945324@qq.com (Q. Zeng), luozhang1759@sohu.com (Z. Luo), huangqunlaoshi@126.com (Q. Huang).
[1] Authors contributed equally to this work.

https://doi.org/10.1016/j.fochx.2022.100541
Received 25 August 2022; Received in revised form 6 December 2022; Accepted 9 December 2022
Available online 15 December 2022

evaluation of food quality and physicochemical indicators such as Total volatile basic nitrogen (TVB-N) (Yang et al., 2017), Thiobarbituric Acid Reactive Substance (TBARS) (Xiong et al., 2015), pH (Dixit, Al-Sarayreh, Craigie, & Reis, 2021), color (Chaudhry et al., 2021), hardness (Zhenjie et al., 2014), tenderness (Barbin, Valous, & Sun, 2013), moisture content (Kamruzzaman, Makino, & Oshita, 2016b), fatty acid content (Ma & Sun, 2020), etc. Also, hyperspectral technology has a broad range of applications in meat products such as lamb (Pu et al., 2014), turkey (Barbin et al., 2020), beef (Kamruzzaman et al., 2016c), chicken (Nolasco-Perez et al., 2019), etc. However, studies using hyperspectral techniques to rapidly assess the freshness of yak meat have not been reported.

However, the predictive power of different chemometric methods also varies. Therefore, the objective of this study was to evaluate the potential of hyperspectral imaging techniques in predicting changes in freshness during yak meat oxidation. The specific aims were to (1) the changes of TVB-N, carbonyl group and surface hydrophobicity during the oxidation of yak meat were investigated to find out the characteristic indexes of freshness of yak meat at different oxidation times; (2) three regression methods: PCR, SVR and PLSR were compared to improve the accuracy of the prediction models; (3) the SPA and CARS methods were used to select the wavelengths associated with the features, build the corresponding regression models and compare their performance; (4) optimal feature wavelengths and prediction models were selected for establishing a system for nondestructive monitoring of freshness changes during yak meat oxidation by hyperspectral imaging. A fast, easy, and non-destructive method for assessing the freshness of yak meat was established in this work, which was critical for quality monitoring of yak meat during processing, storage, and transportation.

2. Materials and methods

2.1. Materials and chemicals

Maiwa yaks (6 females and 6 males) were from the natural pasture of Chuanbei Ge, Ruoerge County, Aba Prefecture, Sichuan Province, China. All yaks were raised in the same pasture under the same standard management conditions, with the same diet, and all yaks were healthy. Yaks were slaughtered by high voltage electric shock at 1000 ± 5 days of age and samples of hind leg meat were collected from yak meat. The hind leg meat was cut into 500 ± 10 g pieces, vacuum packed and quick frozen in −40 °C cold storage, and then transported to our laboratory for frozen storage (−20 °C) on the same day. The samples were thawed at 4 °C for 12 h before use. The yak meat was divided into meat pieces of uniform quality (5 ± 0.1 g) after thawing, cleaning and removing the excess fat and connective tissue. Then, the meat was cleaned with running water, and the water on the surface was dried with paper towels, and then put into a refrigerator at 4 °C for later use.

2.2. Oxidation treatment of yak meat

The pretreated yak meat samples were divided into 12 portions. The water on the surface of the meat was absorbed by paper towels, and the yak meat was oxidized according to the method of Huang et al. (2022). The meat samples were placed in a Fenton oxidation system (1.0 mmol/L $FeCl_3$, 0.1 mmol/L Vitamin C and 10 mmol/L H_2O_2). The ratio of meat samples to oxidizing liquid was 2:1. The meat samples were sealed from light and oxidized for 0, 1, 2, 3, 4, 5, 6, 7, 8, 9, 10, 11 h to obtain different oxidation times. After a period of reaction, EDTA (1.0 mmol/L) was added to chelate Fe^{2+} in the oxidation system to terminate the reaction. The samples were stored in refrigerator at 4 °C for 2 h for later use.

2.3. Characteristics index measurement

2.3.1. TVB-n

Total volatile basic nitrogen (TVB-N) was measured based on the method of Dong et al. (2020) and make appropriate modifications. A total 10 ± 0.1 g of cut samples were homogenised with 100 mL water, shaken for 30 min and then filtered. Add 2 mL of Nessler and 22 mL of water to 1 mL of filtrate, left for 10 min. The absorbance of the sample solution was measured at the wavelength of 420 nm and then the standard curve and the following formula were used to calculate the content of TVB-N (1). Each sample was parallel three times and the average were taken.

$$X = \frac{(C - C_0) \times 10^{-3}}{m \times 1/10 \times V/25} \times 100 \quad (1)$$

where X is the content of volatile base nitrogen in sample (mg/100 g); C is the content of volatile base nitrogen in sample determination solution (μg/mL); C_0 is the volatile base nitrogen in blank determination solution content (μg/mL); m is the sample weight (g); V is the sample volume (mL).

2.3.2. Extraction of myofibrillar protein

The myofibrillar protein (MP) was isolated from yak meat based on the method of Huang et al. (2022) and Liu et al. (2020). The MP were stored in refrigerator at 4 °C. The protein concentration within 48 h was measured by the Biuret method with bovine serum albumin (BSA) used as the standard. The MP concentration was normalised to 10 mg/mL with NaCl phosphate buffer (0.4 mol/L, pH 7.0).

2.3.3. Determination of carbonyl content

The determination of carbonyl content was based on Zhang et al. (2020) method and made some modifications. Take 0.5 mL of myofibrillar proteins solution in a 10 mL centrifuge tube, add 0.2 % DNPH (2 mL) and 2 mol/L HCl (2 mL), and react at room temperature for 1 h. Then add 20 % trichloroacetic acid (2 mL), centrifuge at 10,000 r/min for 10 min, discard the supernatant, and wash the precipitate 3 times with 2 mL of anhydrous ethanol and ethyl acetate (v:v = 1:1). Finally, 6 mol/L guanidine hydrochloride (3 mL) was added to the precipitate, and the precipitate was dissolved in a water bath at 37 °C for 30 min and centrifuged at 10,000 r/min for 10 min to remove the insoluble material, and the absorbance was measured at 370 nm with a spectrophotometer. The carbonyl content was calculated according to Eq. (2). Each sample was parallel three times and the average were taken.

$$\text{The carbonyl content(nmol/mg)} = \frac{A \times 3000,000,000}{\varepsilon \times 2500} \quad (2)$$

where A is the absorbance; ε is the molar absorbance coefficient.

2.3.4. Surface hydrophobicity

The determination of surface hydrophobicity was measured according to the method of Huang et al. (2022) and make some modifications. Myofibrillar protein solution with the concentration of 1 mg/mL was prepared. Take l mL of MP solution, 200 μL of bromophenol blue (1 mg/mL) was add, mixed adequately and shook on a shaker at room temperature for 10 min. Then the solution was centrifuged at 7000xg for 15 min (4 °C), and the supernatant was diluted 10 times. The absorbance value was measured at 595 nm (A). The combination of deionized water and bromophenol blue was used as a blank control (A_0). The surface hydrophobicity is calculated according to Eq. (3):

$$\text{Surface hydrophobicity (ug)} = \frac{200\,\text{ug} \times (A_0 - A)}{A_0} \quad (3)$$

2.4. Hyperspectral image acquisition and processing

2.4.1. Hyperspectral image capture

For each different oxidation time, 15 meat samples were selected and placed on the sample stage. Scanning was performed with a hyperspectral imaging system, and the hyperspectral data were collected and stored using HyoerScanner V2.0r software. The SOC710VP imaging spectrometer (Anzhou Technology Co., Ltd., Beijing, China) with a wavelength range of 400–1000 nm (128 bands) and a resolution of 4.69 nm was used in this experiment (Fig. 2a). The hyperspectral imaging system allowed adjustment of the illumination intensity using the halogen lamp light source on to the sample. The whole acquisition process was performed in a dark room.

2.4.2. Image calibration

The hyperspectral imaging system needs to be warmed up for half an hour before the start of the experiment. Because of instability such as current, the image will generate some noise. So the hyperspectral image needs to be corrected in black and white before sample acquisition. A standard whiteboard was placed on the acquisition platform to obtain the whiteboard data I_W. An opaque cover was used to cover the camera lens to obtain the all-black image I_D. And the yak meat sample was placed on the acquisition platform to obtain the original hyperspectral diffuse reflectance image I_R. The image of yak meat (I) after the calibration was obtained according to Eq. (4) (Ma, Sun, Pu, Cheng, & Wei, 2019):

$$I = \frac{I_R - I_D}{I_W - I_D} \times 100\% \tag{4}$$

2.4.3. ROI identification and spectrum extraction

After image acquisition and calibration, we can easily find the sample area of yak meat using the difference between the meat sample and the background spectrum. However, there might be specular reflections at several pixel points because the surface of the meat sample is not smooth, and these pixel points can have a great impact on the later predictions. Therefore, these pixel points need to be removed when selecting the region of interest. Regions of interest (ROI) were delineated using the rectangle tool in ENVI software. Five ROIs were selected for each sample, and the average spectral reflectance of the selected pixel points was finally taken as the average spectrum of the whole sample. All the extracted spectral informations were saved in the form of a matrix, where column X represents the wavelength and column Y represents the sample. All subsequent image processing operations were performed on these ROIs. Spectral information was extracted from the hyperspectral images using ENVI 4.8 (ITT Visual Information Solutions, Boulder, CO, USA).

2.4.4. Spectral data processing

2.4.4.1. Rational division of the sample set. Prior to data analysis of the samples, the entire data set (180 samples) was divided into a sample set and a prediction set. The selection of representative sample sets and prediction set samples was the basis for building the stability model. The selection of samples not only affects the prediction accuracy of the model, but also has a great influence on the stability of the model. The commonly used sample partitioning algorithms mainly include Kennard-Stone (KS) (Kucha et al., 2021) and Sample Set Partitioning Based on Joint X-Y Distance (SPXY) (Fan et al., 2021). Among them, a total of 134 correction sets and 46 prediction sets were selected based on the KS algorithm. 135 correction sets and 45 prediction sets were selected based on SPXY algorithm. The sample division was implemented using a self-developed program in JetBrains PyCharm 2019.

2.4.4.2. Spectral pre-processing. In the process of collecting spectra, it was easy to be affected by dark currents, voltages, vibrations, devices, etc., which made the collected spectra might contain more useless information. Therefore, large spectral data which contain a lot of hidden information need to choose a reasonable spectral pre-processing method to eliminate the redundant information. So that the accuracy and stability of the model can be improved. It was very important to pre-process the spectra before modeling. The common spectral pre-processing methods include Moving average (MA), Savitzky-Golay (SG) (Kamruzzaman et al., 2016b), Normalize (Nor) (Wang et al., 2020), Multivariate Scatter calibration (MSC) (Xiong et al., 2015), Standard Normal Variable transformation (SNV) (Kucha et al., 2021), etc.

2.4.4.3. Selection of characteristic wavelength. There were 128 bands of spectral data in the original spectral data. And its data volume and computation were great in quantity, which was not conducive to the construction and application of the model. Therefore, the feature wavelength with the highest contribution from all the spectral band data needed to be selected for modeling. This not only reduces the complexity of the model, but also improves the stability and prediction accuracy of the model. The commonly used feature wavelength selection algorithms include Successive Projection Algorithm (SPA) (Cheng, Sun, Pu, & Liu, 2016), Competitive Adaptive Reweighted Sampling (CARS) (Fan et al., 2021). The feature wavelength selection was implemented based on a self-developed program in Matlab R2016a software (The Mathworks Inc., Natick, MA, USA).

In this study, the full-band spectra contained a larger amount of spectral information, with a large number of bands and the cumbersome data. This not only reduced the efficiency of model calculation, but also discouraged the application of spectral models in daily life. Therefore, SPA and CARS methods were used for the selection of characteristic wavelengths for full-band spectral data.

2.4.5. Modeling method

After processing the spectral information, a reliable multivariate data analysis method needed to be selected to build a mathematical calibration model for quantitative or qualitative analysis. The most common methods used to analyze meat hyperspectral data include: PCR (Amit et al., 2020), SVR (Leng et al., 2021), PLSR (Cheng, Sørensen, Engelsen, Sun, & Pu, 2019), etc. These methods all combined hyperspectral data and reference measurements of physicochemical indicators to provide predictive values for the physicochemical indicators of interest using their representative data sets. Because these models require representative data, a large number of samples containing the expected changes in the physicochemical indicators of the samples being monitored were required.

The PCR is one of the most basic and common used algorithms in pattern recognition algorithms. It extracts the intrinsic features between data by linear variation (Rodriguez-Nogales, 2006). The SVR is a powerful machine learning algorithm which can transform the input set of samples into a high-dimensional space, resulting in a better separation of the data (Yao et al., 2019). As a new multivariate statistical data analysis method, PLSR combines the advantages of models such as correlation analysis, principal component analysis and multiple linear regression, which has a broader scope of application, better analysis of effects, stronger explanatory power and higher accuracy (Kucha, Liu, Ngadi, & Claude, 2021).

This study focused on developing hyperspectral models for yak meat freshness identification, comparing the modeling effects of three models such as PCR, SVR and PLSR, and selecting the optimal spectral model.

2.4.6. Model evaluation indexes

The performance of the regression model was evaluated using statistical criteria, mainly the correlation coefficient R_c^2 and root mean square error RMSEC for the calibration set, the correlation coefficient R_p^2 and root mean square error RMSEP for the prediction set, and the residual prediction deviation RPD. A correlation coefficient closer to 1 and

a root mean square error closer to 0 indicate that the model is more predictive and stable. RPD was generally used to evaluate the accuracy and precision of the model (Pu et al., 2014). RPD was the ratio of standard deviation and root mean square error, which proved the usefulness of the model. A higher RPD value indicated that the model was able to predict the chemical composition accurately. All model building and analysis was done by using The Unscrambler X10.4 (CAMO Software, Oslo, Norway) software.

3. Results and discussion

3.1. Analysis of characteristic index results

In order to obtain better freshness prediction results, samples of yak meat were selected for freshness indexes at 12 time periods with the extension of oxidation time. The best correlation with oxidation time was selected from many indicators by using significance and correlation. Then the prediction model of yak meat freshness index was established.

TVB-N value was one of the important indicator to evaluate the freshness of meat products (Dong et al., 2020). As seen in Fig. 1a, the TVB-N value in yak meat increased significantly ($P < 0.01$) with the increase of oxidation time, which was positively correlated with the degree of spoilage of yak meat. When the oxidation time was 2 h, the TVB-N value exceeded the Chinese standard for first grade fresh meat (15 mg/100 g). When the oxidation time was 7 h, the TVB-N content exceeded 20 mg/100 g, which belongs to spoiled meat. During the oxidation process of yak meat, proteins were gradually oxidized and degraded, the structural integrity of muscle cells was destroyed. The protein degradation led to the release of a large number of enzymes, which in turn accelerated the degradation of proteins, the decomposition of amino acids and the release of metabolites (Luo et al., 2021).

Carbonyl groups were used to measure the degree of protein oxidation, generally. During the oxidation process, the carbonyl content of yak beef myofibrillar proteins showed a general trend of increasing and then decreasing, and reached a maximum value of 1.3121 nmol/g at 6 h (Fig. 1b). The increase in carbonyl content was due to the fact that some amino acids carried by the side chains of the protein backbone were easily converted to carbonyl groups during oxidation (Xin et al., 2021). The carbonyl content decreased after 6 h because the newly formed carbonyl group would attack the nucleophilic material in the protein, thus causing the carbonyl ammonia condensation reaction (Huang et al., 2022).

The surface hydrophobicity of the protein has a great influence on the functional properties of the protein, and expressed as the amount of binding to bromophenol blue generally. With the increase of oxidation time, the surface hydrophobicity showed a general trend of increasing and then decreasing (Fig. 1c). It might be due to the folding of protein molecules after protein oxidation, where the molecular conformation of the protein was changed to expose more hydrophobic groups (Huang, Sun, Liu, et al., 2022). However, with the increase of oxidation time, the protein molecules underwent aggregation and cross-linking between side chains. Some hydrophobic groups were re-embedded inside the protein, causing the reduction of surface hydrophobicity (Liu et al., 2021).

3.2. Freshness feature index screening

During the oxidation process, TVB-N, carbonyl content and surface hydrophobicity of yak meat were analyzed for correlation. And the correlation coefficients between the variables were determined by using the Pearson function. Person's correlation coefficient ranges from −1.0 to 1.0, and the absolute value of the correlation coefficient indicated the degree of correlation between the two variables (Junkui et al., 2020). The TVB-N values were negatively correlated with storage time. The correlation coefficient of TVB-N, carbonyl content, surface hydrophobicity was 0.9952, 0.4962, 0.4813, respectively. The correlation coefficients were found to be greater than 0.8 for TVB-N values. Therefore, in this study, TVB-N value were selected as a characteristic indicator of freshness of yak beef at different oxidation time, taking into account the significance and correlation coefficients. The correlation analysis was calculated and analyzed through SPSS 18.0 software (SPSS Inc., Chicago, IL, USA).

3.3. Spectral data pre-processing

The average raw spectra (400–1000 nm) of yak meat for different oxidation times (0 h, 1 h, 2 h, 3 h, 4 h, 5 h, 6 h, 7 h, 8 h, 9 h, 10 h and 11 h) were shown in Fig. 2b. Yak meat spectra exhibited typical spectral features of meat tissues, mainly characterized by vibrational signals of proteins, lipids and water. Several absorption bands can be clearly identified in the average raw spectrum, which were mainly distributed at 430 nm, 540 nm, 730 nm and 970 nm. The absorption peaks located at 430 nm may be related to hemoglobin chemical bond vibrations (Yang et al., 2017). 540 nm and 575 nm absorption peaks may be related to deoxy-myoglobin and oxidized myoglobin (Kamruzzaman et al., 2016b). The absorption peaks at both 730 nm and 970 nm were clearly caused by triplet and diphasic absorption of O—H bonds in water molecules (Kamruzzaman, Makino, & Oshita, 2016a). The absorption peak observed near 1024 nm can be attributed to the second overtone of protein N—H stretching (Patel, Toledo-Alvarado, & Bittante, 2021). As can be seen in Fig. 2, yak meat samples with different oxidation times basically showed the same trend. But there were some differences in the spectral intensities of the different samples, and their freshness could not be directly identified. So the freshness of yak meat needs to be predicted by building a corresponding model on the spectral data.

3.4. Full-wavelength-based modeling

3.4.1. Sample set division

In order to ensure the accuracy of the model, the spectral set needed to be reasonably divided. The relative Euclidean distances between the variable spaces were used to divide the sample sets and find out the samples with large gaps and selected them into the calibration set (Gao, Wang, Qing-Xu, Shi, & University, 2019). Samples with a large

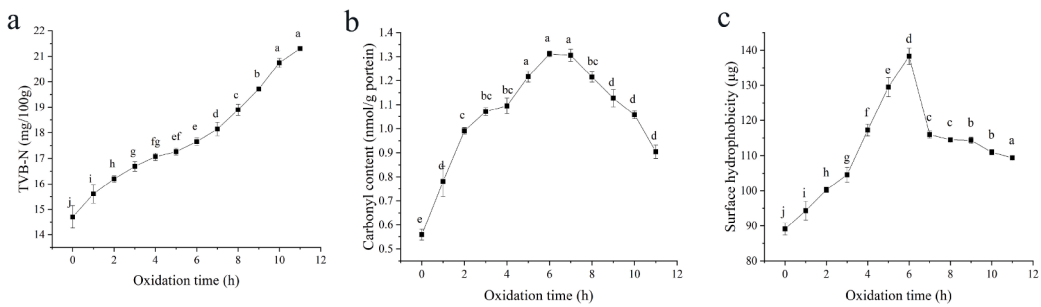

Fig. 1. Effect of different oxidation times on the physicochemical index of yak meat. (a:TVB-N and carbonyl, b: total sulfhydryl and surface hydrophobicity).

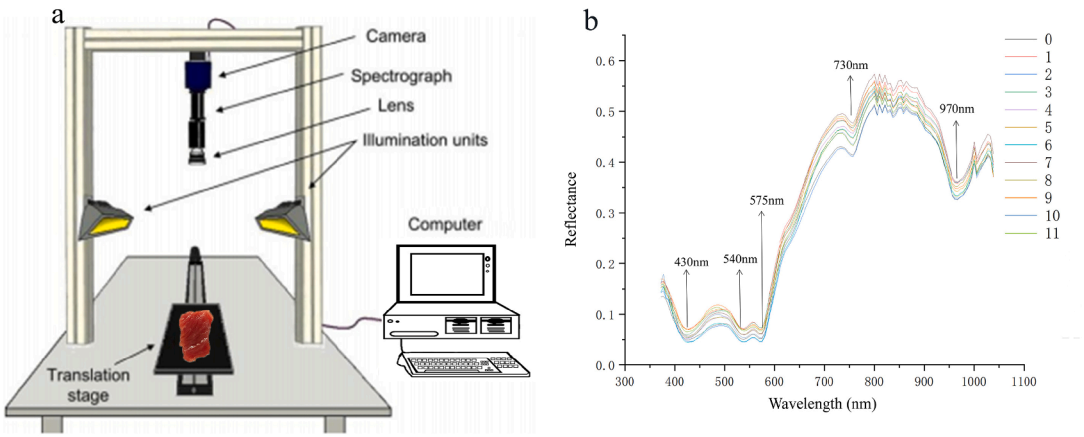

Fig. 2. Schematic diagrams of main components of the hyperspectral imaging system (a) and average raw spectra of yak meat samples at different oxidation times (b).

difference in Euclidean distance were selected into the calibration set, and those with a similar distance were selected into the prediction set. The PLSR calibration model was established based on the original spectra. As shown in Table 1, after the samples were divided by SPXY, the TVB-N content model showed good prediction ability, in which the ratio of Prediction to Deviation (RPD) was as high as 2.3082, indicating that the model was stable and accurate.

3.4.2. *Prediction ability of PCR model*

During the acquisition process, the spectral information has some redundant information that was not such elevant to the nature of the sample itself due to the influence of the external environment. The redundant information had a great impact on the stability and predictability of the model. Therefore, five different pre-processing methods (MA, SG, Nor, MSC, SNV) were used to deal with the raw spectra. A quantitative model was developed by PCR regression algorithm, and the validation set was substituted into the model for predictive power assessment. The results were shown in Table 1.

As shown in Table 1, the original spectra were treated with MA and MSC, and although the R_c^2 values increased slightly, the R_p^2 values decreased significantly. For both spectral preprocessing methods, although the R_c^2 values reached 0.8901 and 0.8941, the R_p^2 was only 0.7787 and 0.7765. The large difference between the R_c^2 and R_p^2 values may because of model over-fitting and thus model performance degradation.

The raw spectra all had different degrees of improvement in R_c^2 values after pre-processing. However, the accuracy of the model was not effectively extracted by every pre-processing method. The correlation coefficients R_c^2 for the calibration set and R_p^2 for the prediction set of the model were built after the original spectra were processed by SG in the PCR processing model were 0.9082 and 0.8409, the result was shown in Table 1. The results were significantly higher than the models built by other pre-processing methods, and the root mean square error of both their calibration and prediction sets were smaller. Therefore, SG was determined to be the best pre-processing method for the spectra, and the PCR model for the characteristic wavelengths was built according to the SG pre-processing spectral data.

The scatter plots of the actual and predicted values of TVB-N content of yak meat during model calibration and validation were shown in Fig. 3a. PCR models were built by using the raw spectra data after SG

Table 1
The influence of different pretreatment methods on the PCR, SVR and PLSR model based on full wavelength.

Model	Pretreatment methods	Factors	Calibration		Prediction		RPD
			R_c^2	RMSEC	R^2p	RMSEP	
PLSR + TVB-N	KS	8	0.8579	1.1631	0.8046	1.3274	1.5688
	SPXY	7	0.8639	1.1385	0.8595	1.1401	2.3082
PCR + TVB-N + SPXY	None	8	0.8542	1.1725	0.7820	1.4761	2.0358
	MA	8	0.8901	1.1684	0.7787	1.5022	2.0005
	SG	8	0.9082	1.0359	0.8409	1.2088	2.4860
	Nor	7	0.8894	1.1392	0.8262	1.3505	2.2252
	MSC	7	0.8941	1.1284	0.7765	1.5134	1.9872
	SNV	7	0.8824	1.2697	0.8349	1.2873	2.3344
SVR + TVB-N + SPXY	None	–	0.8562	1.2649	0.6805	1.4658	2.0501
	MA	–	0.8524	1.2732	0.6738	1.4888	2.0185
	SG	–	0.8529	1.2701	0.6742	1.4959	2.0089
	Nor	–	0.8929	1.1457	0.7138	1.4035	2.1411
	MSC	–	0.8931	1.1417	0.7569	1.3621	2.2062
	SNV	–	0.9128	0.9611	0.8068	1.3236	2.2704
PLSR + TVB-N + SPXY	None	9	0.8639	1.1385	0.8595	1.1401	2.3082
	MA	8	0.8628	1.0988	0.8617	1.1254	2.6703
	SG	9	0.9199	0.9494	0.8708	1.0665	2.8177
	Nor	8	0.8888	0.9828	0.8534	1.1234	2.6750
	MSC	7	0.9058	1.0173	0.8689	1.1364	2.6444
	SNV	7	0.8900	1.0013	0.8699	1.0913	2.7537

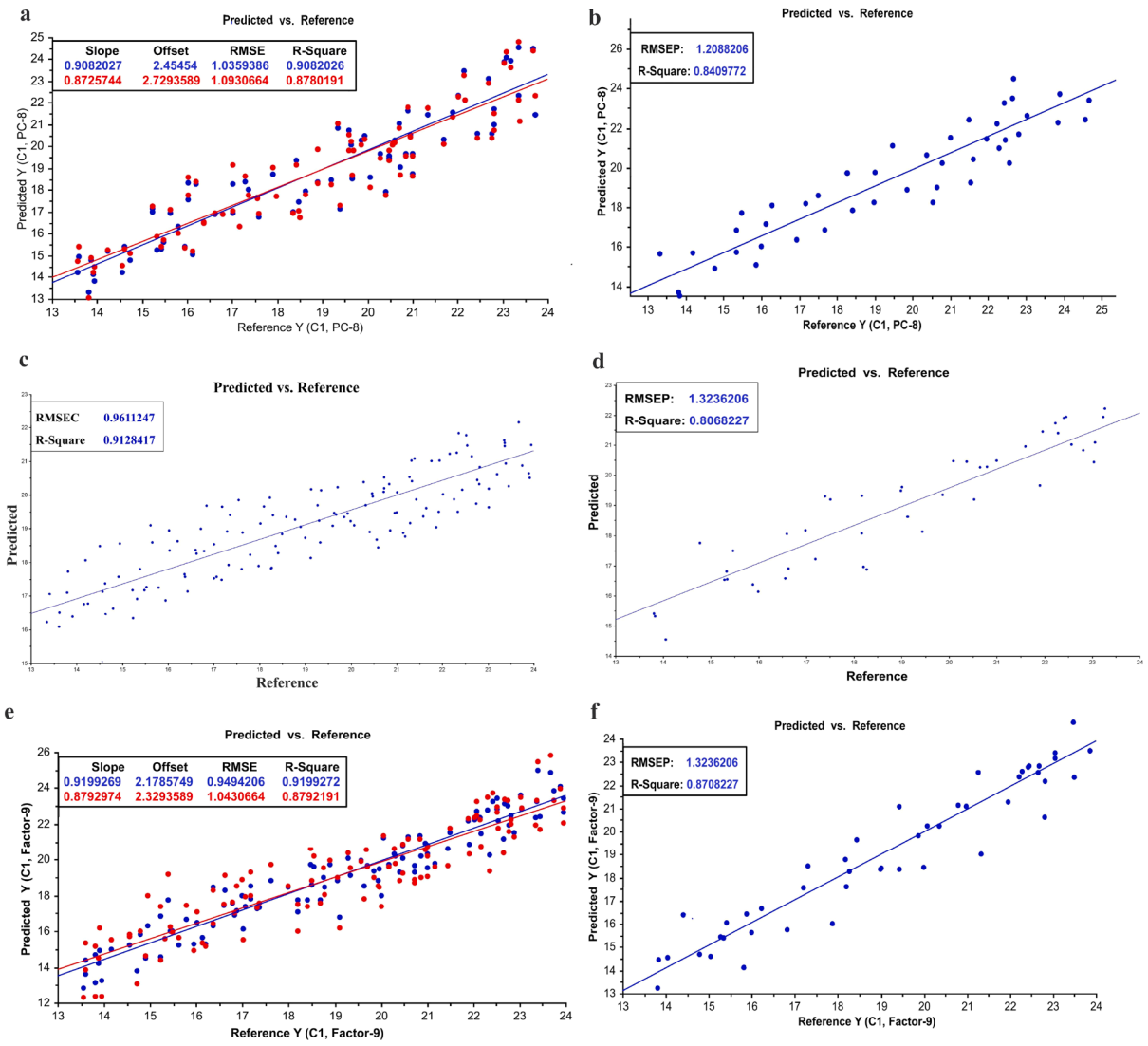

Fig. 3. Scatter plot result of PCR (a and b), SVR (c and d) and PLSR (e and f) model.

processing, and the final result was obtained with the validation set R_c^2 = 0.9082 and RMSEC = 1.0359. All sample points were evenly distributed on both sides of the ideal line when the PCR model was evaluated by using samples from the prediction set, where $R_p^2 = 0.8409$ and RMSEP = 1.2088 (Fig. 3b). The results indicated that it was feasible to use PCR model to detect TVB-N content in yak meat.

3.4.3. Prediction ability of SVR model

Nonlinear SVR models based on the original spectra were built through five pre-processing methods. The performance of the models built based on the five pre-processing techniques above was shown in Table 1. Similar to the PCR model, the SVR model built from the original spectra after SNV processing had a higher R_c^2 and lower RMSEC (R_c^2 = 0.9128, RMSEC = 0.9611) compared to other pre-processing methods. And the correlation coefficient of the prediction set was significantly larger and the root mean square error was significantly decline. The original spectra were processed by SNV to remove most of the useless feature information, and the established SVR model achieved the best results. The scatter plots of the actual and predicted values of the SVR model constructed based on the full spectral range for the TVB-N content of yak meat were shown in Fig. 3c and Fig. 3d. The results showed that it was feasible to detect TVB-N content in yak meat by SVR model. And then, the SNV pre-processed spectral data was used to extract the feature wavelengths and establish SVR model.

3.4.4. Prediction ability of PLSR model

In this study, five different spectral pre-processing techniques were used to build a full-spectrum-based PLSR model. Table 1 indicated the effects of different pretreatment methods on the performance of the full-wavelength PLSR model. As can be seen from Table 1, the correlation coefficients of the prediction set of the PLSR model built after pre-treatment of the original spectra significantly increased. The root mean square error significantly decreased, and the RPD significantly increased compared with the model built from the original spectra. The result indicated that the PLSR model built after some pretreatment of the original spectra achieved better performance. For the TVB-N values, the optimization of the raw spectra depend on SG led to better results with R_c^2 of 0.9199 and R_p^2 of 0.8708, both of which were significantly greater than the other pre-processing methods. The scatter plots and predicted plots of the PLSR model built based on the full spectrum were shown in Fig. 3e and Fig. 3f. The results showed that it was feasible to detect the TVB-N content in yak meat by PLSR model, and the extraction of feature wavelengths and the PLSR model built in the following were according to the spectral data pre-processed by SG.

3.4.5. Comparison of PCR, SVR and PLSR models

In this study, the prediction models of TVB-N values during yak meat oxidation were constructed by PCR, SVR and PLSR models, respectively. The results showed that the nonlinear SVR model failed to produce

satisfactory results in the prediction model of TVB-N values. In contrast, PLSR, as a powerful multiple linear regression method, was more suitable for prediction with TVB-N values. It was well known that the true predictive power of any calibrated model must be validated against the predictions of samples not included in the calibration test. The best model obtained from PLSR, after the raw spectra data were processed by SG ($R_p^2 = 0.8708$), which was much larger than the $R_p^2 = 0.8068$ of the SVR model. And the RMSEP = 1.0655 of the PLSR model was much lower than the RMSEP = 1.3236 of the SVR model. The closer the RMSEP value was to 0, the higher the model accuracy and the better the stability. In general, the PLSR model had better model accuracy and model stability than the PCR and SVR models. These results also indicated that the PLSR linear regression method provided the best results compared to other multivariate calibration methods, which was also similar to the results of Leng et al. (2021). This study demonstrated that PLSR regression method was superior in predicting the TVB-N content of yak meat.

3.5. Extraction of characteristic wavelengths

Taking the extraction of feature wavelengths by SPA as an example, the number of feature wavelengths was set to range from 1 to 12, and the step size was 1. According to the principle of SPA, the Root Mean Square Error of Cross Validation (RMSECV) was used to determine the stability and accuracy of the model, and the smaller the RMSECV, the better the stability of the model and the higher the accuracy. The RMSECV declined rapidly as the number of characteristic wavelengths increased, and the RMSECV achieved the minimum value when the number of characteristic wavelengths reached to 9 (Fig. 4b). Meanwhile, in order to reduce the complexity of the model, the characteristic wavelengths were selected according to the principle of minimum RMSECV: 442.6, 472.9, 575.0, 726.0, 752.4, 816.1, 832.2, 976.3, 1027.6. A total of nine characteristic wavelengths were selected, and the index of the selected wavelength points in the original spectrum was shown in Fig. 4a. The selected bands accounted for 7.031 % of the original spectral information.

Similar to the SPA-based feature wavelength selection modeling, the raw spectra were processed and then the feature wavelengths were extracted by CARS algorithm. As shown in the Fig. 4d, the number of Monte Carlo samples was set to 50, and the 5-fold cross-validation method was used for the calculation. It indicated that useless information was removed from the spectral data when the RMSECV value gradually decreased, and when it gradually increased, it showed that useful and important information was removed from the spectral data. The results showed that the RMSECV value reduced and then augmented with the increase of sampling times. And the RMSECV obtained the minimum value when the sampling times were run to 27 times. At a same time, a total of 11 characteristic wavelengths were screened, and the selected characteristic wavelengths accounted for 8.594 % of the original spectral information. The characteristic wavelengths were shown in Fig. 4c, 422.5, 483.0, 544.2, 559.6, 575.0, 726.0, 752.4, 832.2, 972.7, 1016.6, 1033.1.

3.6. Feature wavelength-based modeling

Similar to the full-wavelength-based modeling approach, the PCR, SVR, and PLSR were modeled with 9 characteristic wavelengths by SPA and 11 characteristic wavelengths by CARS, respectively. The statistical results were listed in Table 2. It can be seen that the stability and prediction accuracy of the model on account of the characteristic wavelengths were improved compared with the model developed using the full wavelengths. The results indicated that the regression model based on the characteristic wavelength has good performance for the prediction of TVB-N content in yak meat. Comparing the stability and prediction accuracy of the PCR, SVR and PLSR models on account of the characteristic wavelength. We found that the PLSR model have better

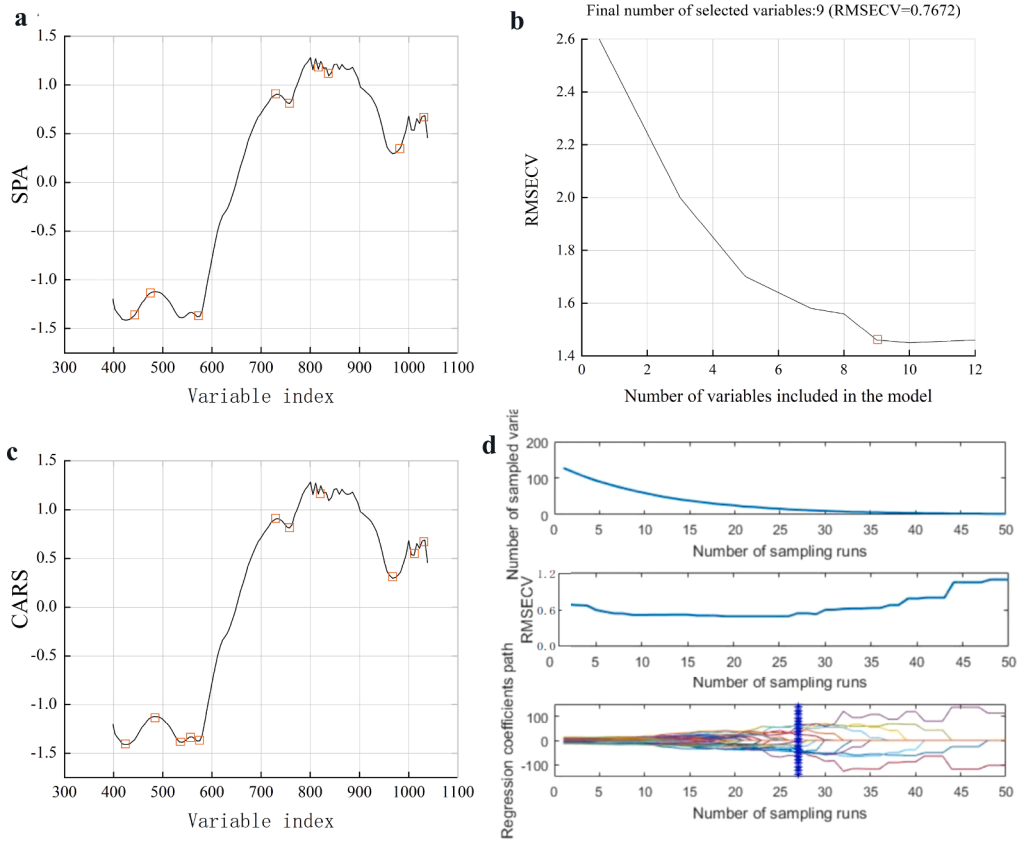

Fig. 4. SPA and CARS characteristic wavelength selection maps (a and c) and RMSECV variation maps (b and d) for TVB-N values of yak meat.

Table 2
The influence of different feature wavelength selection methods on PCR, SVR, and PLSR models.

Model	Pretreatment methods	Factors	Calibration		Prediction		RPD
			R_c^2	RMSEC	R_p^2	RMSEP	
PCR + SG	Full	8	0.9082	1.0359	0.8409	1.2088	2.4860
	SPA	9	0.9125	1.0125	0.8449	1.2995	2.3125
	CARS	7	0.9180	0.9377	0.8837	1.0685	2.8124
SVR + SNV	Full	–	0.9128	0.9611	0.8068	1.3236	2.2704
	SPA	–	0.9201	0.9316	0.8605	1.2495	2.4050
	CARS	–	0.9185	0.9594	0.8192	1.3043	2.3040
PLSR + SG	Full	9	0.9199	0.9494	0.8708	1.0665	2.8177
	SPA	7	0.9305	0.7672	0.9103	0.9243	3.2512
	CARS	6	0.9553	0.5972	0.9206	0.8688	3.4589

performance, higher accuracy and smaller root mean square error than the PCR and SVR models. The R_c^2 and R_p^2 of the PLSR model based on the feature wavelength extracted by the CARS algorithm were 0.9553 and 0.9206, respectively. As well as the R_c^2 and R_p^2 of the PLSR model on account of the feature wavelength extracted by the SPA algorithm were 0.9305 and 0.9103, respectively. The analysis concluded that the model built by the CARS algorithm has better performance, higher prediction and smaller root mean square error than the model built by the SPA algorithm. Meanwhile, the feature wavelengths extracted based on CARS algorithm contain a large amount of effective spectral information, which included the spectral information corresponding to water, protein, fat and other substances in yak meat. Therefore, the PLSR model extracted by CARS algorithm and developed has strong characterization power for TVB-N content and freshness of yak meat, which can be the best model for quality deterioration and TVB-N content in yak meat during oxidation.

Interestingly, we found that the feature wavelengths extracted by the CARS-based algorithms contain three feature wavelengths, 544.2, 559.6, and 575.0 nm. However, these three feature wavelengths were close to each other, because we suspected that these three feature wavelengths were related. Therefore, we needed to further optimize the feature wavelength extraction algorithm and try to reduce the number of feature wavelengths while ensuring the accuracy of the model. This will not only the model can be simplified, but also the hyperspectral system built on the feature wavelengths will be more convenient and faster.

3.7. Comparison of results obtained with other authors

In summary, we found that the PLSR model was greater than the PCR and SVR models in predicting the TVB-N content of yak meat during oxidation. To further evaluate the ability of the PLSR model to predict the TVB-N values in yak meat, we compared and analyzed the results of the PLSR model with those obtained from other literature.

Leng et al. (2021) applied PLSR and SVR regression models to develop a quantitative model for predicting TVB-N content in beef and pork by near-infrared diffuse reflectance spectroscopy. The best PLSR model based on the raw spectra showed excellent prediction performance with correlation coefficient values as high as 0.9366, which was similar to our results. However, the PLSR model that we developed to predict the TVB-N content of yak meat on account of the characteristic wavelength had a correlation coefficient as high as 0.9553, and its prediction accuracy was slightly higher than that of the study by Leng et al. It might be that Leng et al. selected 383 characteristic wavelengths from 909 wavelengths, however the number of selected characteristic wavelengths was relatively large, which still had more useless spectral information.

Meanwhile, Yang et al. (2017) developed a model for nondestructive detection of TVB-N content in cured meat during drying using a hyperspectral imaging system (HSI). The results indicated that the PLSR model on account of the full wavelength produced acceptable predictions of TVB-N content ($R_c^2 = 0.915$, $R_p^2 = 0.853$). Their prediction was lower than ours probably because they had fewer sample classification methods and pre-processing methods, so they was failed to find the best spectral processing method.

Overall, we developed a quantitative PLSR model for TVB-N content in yak meat during oxidation using hyperspectral techniques combined with chemometric methods. And we obtained better model accuracy ($R_c^2 = 0.9553$) and model prediction ($R_p^2 = 0.9206$). Our results also confirmed the great potential of hyperspectral techniques for the nondestructive detection of TVB-N content in yak meat.

4. Conclusion

Hyperspectral techniques were applied for the first time to construct a content prediction model for yak meat freshness (TVB-N value) index in the wavelength range of 400–1000 nm during the oxidation process. The results indicated that the full-wavelength based PCR, SVR, and PLSR models were shown greater performance in the prediction of TVB-N content. Among them, the PLSR model showed best stability and model accuracy ($R_c^2 = 0.9199$, $R_p^2 = 0.8708$). Furthermore, in order to improved the efficiency of the model operation and decreased the dimensionality of the original spectral matrix, 9 and 11 characteristic wavelengths were extracted from 128 wavelengths by SPA and CARS algorithm, respectively. The simplified CARS-PLSR model showed better results ($R_c^2 = 0.9553$, $R_p^2 = 0.9206$) in evaluation of TVB-N content during yak meat oxidation. This research provided a simple and rapid method for detecting changes in freshness of yak meat during the oxidation process. In addition, more advanced spectral pre-processing methods and modeling approaches need to be explored to build models with better predictive capabilities.

CRediT authorship contribution statement

Kai Dong: Investigation, Formal analysis, Writing – original draft, Writing – review & editing. **Yufang Guan:** Investigation, Formal analysis, Writing – original draft, Writing – review & editing. **Qia Wang:** Investigation, Methodology, Formal analysis. **Yonghui Huang:** Validation, Investigation. **Fengping An:** Data curation, Software. **Qibing Zeng:** Funding acquisition, Conceptualization. **Zhang Luo:** Funding acquisition, Supervision. **Qun Huang:** Validation, Supervision.

Declaration of Competing Interest

The authors declare that they have no known competing financial interests or personal relationships that could have appeared to influence the work reported in this paper.

Data availability

No data was used for the research described in the article.

Acknowledgements

This study was financially supported through grants from the Open Foundation for Key Laboratory of Environmental Pollution Monitoring and Disease Control, Ministry of Education (No. KY[2022] 384), Foundation of Guizhou Educational Committee (No. KY [2021] 008 and No. KY [2020] 014) and Central Support Special Fund for the Reform and Development of Tibet Local Colleges and Universities (503118004).

Data Availability

Research data are not shared.

Ethical Guidelines

All procedures were performed in compliance with relevant laws and institutional guidelines and ethics approval was not required for this research.

References

Amit, Jamwal, R., Kumari, S., Kelly, S., Cannavan, A., & Singh, D. K. (2020). Rapid detection of pure coconut oil adulteration with fried coconut oil using ATR-FTIR spectroscopy coupled with multivariate regression modelling. Lwt-Food Science and Technology, 125, 109250, doi: 10.1016/j.lwt.2020.109250.

Baek, I., Lee, H., Cho, B.-K., Mo, C., Chan, D. E., & Kim, M. S. (2021). Shortwave infrared hyperspectral imaging system coupled with multivariable method for TVB-N measurement in pork. *Food Control, 124*, Article 107854. https://doi.org/10.1016/j.foodcont.2020.107854

Barbin, D. F., Valous, N. A., & Sun, D. W. (2013). Tenderness prediction in porcine longissimus dorsi muscles using instrumental measurements along with NIR hyperspectral and computer vision imagery. *Innovative Food Science & Emerging Technologies, 20*, 335–342. https://doi.org/10.1016/j.ifset.2013.07.005

Barbin, D. F., Badaró, A. T., Honorato, D. C. B., Ida, E. Y., & Shimokomaki, M. (2020). Identification of turkey meat and processed products using near infrared spectroscopy. *Food Control, 107*, Article 106816. https://doi.org/10.1016/j.foodcont.2019.106816

Casaburi, A., Piombino, P., Nychas, G.-J., Villani, F., & Ercolini, D. (2015). Bacterial populations and the volatilome associated to meat spoilage. *Food Microbiology, 45*, 83–102. https://doi.org/10.1016/j.fm.2014.02.002

Chaudhry, M. M. A., Hasan, M. M., Erkinbaev, C., Paliwal, J., Suman, S., & Rodas-Gonzalez, A. (2021). Bison muscle discrimination and color stability prediction using near-infrared hyperspectral imaging. *Biosystems Engineering, 209*, 1–13. https://doi.org/10.1016/j.biosystemseng.2021.06.010

Cheng, W., Sun, D.-W., Pu, H., & Liu, Y. (2016). Integration of spectral and textural data for enhancing hyperspectral prediction of K value in pork meat. *LWT - Food Science and Technology, 72*, 322–329. https://doi.org/10.1016/j.lwt.2016.05.003

Dixit, Y., Al-Sarayreh, M., Craigie, C. R., & Reis, M. M. (2021). A global calibration model for prediction of intramuscular fat and pH in red meat using hyperspectral imaging. *Meat Science, 181*, Article 108405. https://doi.org/10.1016/j.meatsci.2020.108405

Dong, K., Luo, X., Liu, L., An, F., Tang, D., Fu, L., & Huang, Q. (2020). Effect of high-pressure treatment on the quality of prepared chicken breast. *International Journal of Food Science & Technology, 56*, 1597–1607. https://doi.org/10.1111/ijfs.14776

Fan, N., Ma, X., Liu, G., Ban, J., Yuan, R., & Sun, Y. (2021). Rapid determination of TBARS content by hyperspectral imaging for evaluating lipid oxidation in mutton. *Journal of Food Composition and Analysis, 103*, Article 104110. https://doi.org/10.1016/j.jfca.2021.104110

Gao, S., Wang, Q. H., Qing-Xu, L. I., Shi, H., & University, H. A. (2019). Non-destructive detection of vitamin C, sugar content and total acidity of red globe grape based on near-infrared spectroscopy. Chinese Journal of Analytical Chemistry. 2019, 47(6): 941-949, doi: 10.19756/j.issn.0253-3820.191124.

Huang, Q., Dong, K., Wang, Q., Huang, X., Wang, G., An, F., & Luo, P. (2022). Changes in volatile flavor of yak meat during oxidation based on multi-omics. *Food Chemistry, 371*, Article 131103. https://doi.org/10.1016/j.foodchem.2021.131103

Huang, Q., Liu, L., Wu, Y. Y., Huang, X., Wang, G. Z., Song, H. B., & Luo, P. (2022). Mechanism of differences in characteristics of thick/thin egg whites during storage: Physicochemical, functional and molecular structure characteristics analysis. *Food Chemistry, 369*, Article 130828. https://doi.org/10.1016/j.foodchem.2021.130828

Huang, X., Sun, L., Liu, L., Wang, G., Luo, P., Tang, D., & Huang, Q. (2022). Study on the mechanism of mulberry polyphenols inhibiting oxidation of beef myofibrillar protein. *Food Chemistry, 372*, Article 131241. https://doi.org/10.1016/j.foodchem.2021.131241

Junkui, L., Liming, L., Xiaoyu, L., Tianzhen, W., Xiaojing, Y., Xiaobo, Z., & Zongbao, S. (2020). Detection of freshness indexes of imported chilled beef using hyperspectral imaging technology. *Food Science, 41*(22), 315–323. https://doi.org/10.7506/spkx1002-6630-20191005-002

Kamruzzaman, M., Makino, Y., & Oshita, S. (2016a). Hyperspectral imaging for real-time monitoring of water holding capacity in red meat. *LWT - Food Science and Technology, 66*, 685–691. https://doi.org/10.1016/j.lwt.2015.11.021

Kamruzzaman, M., Makino, Y., & Oshita, S. (2016b). Parsimonious model development for real-time monitoring of moisture in red meat using hyperspectral imaging. *Food Chemistry, 196*, 1084–1091. https://doi.org/10.1016/j.foodchem.2015.10.051

Kamruzzaman, M., Makino, Y., & Oshita, S. (2016c). Online monitoring of red meat color using hyperspectral imaging. *Meat Science, 116*, 110–117. https://doi.org/10.1016/j.meatsci.2016.02.004

Kucha, C. T., Liu, L., Ngadi, M., & Claude, G. (2021). Hyperspectral imaging and chemometrics as a non-invasive tool to discriminate and analyze iodine value of pork fat. *Food Control, 127*, Article 108145. https://doi.org/10.1016/j.foodcont.2021.108145

Leng, T., Li, F., Chen, Y., Tang, L., Xie, J., & Yu, Q. (2021). Fast quantification of total volatile basic nitrogen (TVB-N) content in beef and pork by near-infrared spectroscopy: Comparison of SVR and PLS model. *Meat Science, 180*, Article 108559. https://doi.org/10.1016/j.meatsci.2021.108559

Liu, T., Zhang, W., Yuwono, M., Zhang, M., Ueland, M., Forbes, S. L., & Su, S. W. (2020). A data-driven meat freshness monitoring and evaluation method using rapid centroid estimation and hidden Markov models. *Sensors and Actuators B: Chemical, 311*, Article 127868. https://doi.org/10.1016/j.snb.2020.127868

Liu, X., Wang, J., Huang, Q., Cheng, L., Gan, R., Liu, L., & Geng, F. (2020). Underlying mechanism for the differences in heat-induced gel properties between thick egg whites and thin egg whites: Gel properties, structure and quantitative proteome analysis. *Food Hydrocolloids, 106*, Article 105873. https://doi.org/10.1016/j.foodhyd.2020.105873

Liu, X., Wang, J., Liu, L., Cheng, L., Huang, Q., Wu, D., & Geng, F. (2021). Quantitative N-glycoproteomic analyses provide insights into the effects of thermal processes on egg white functional properties. *Food Chemistry, 342*, Article 128252. https://doi.org/10.1016/j.foodchem.2020.128252

Luo, X., Dong, K., Liu, L., An, F., Tang, D., Fu, L., Huang, Q. (2021). Proteins associated with quality deterioration of prepared chicken breast based on differential proteomics during refrigerated storage. Journal of the Science of Food and Agriculture, 101, 3489-3499, doi: 10.1002/jsfa.10980.

Ma, J., & Sun, D. W. (2020). Prediction of monounsaturated and polyunsaturated fatty acids of various processed pork meats using improved hyperspectral imaging technique. *Food Chemistry, 321*, Article 126695. https://doi.org/10.1016/j.foodchem.2020.126695

Ma, J., Sun, D. W., Pu, H., Cheng, J. H., & Wei, Q. (2019). Advanced techniques for hyperspectral imaging in the food industry: principles and recent applications. *Annual Review of Food Science and Technology, 10*, 197–220. https://doi.org/10.1146/annurev-food-032818-121155

Nolasco-Perez, I. M., Rocco, L. A. C. M., Cruz-Tirado, J. P., Pollonio, M. A. R., Barbon, S., Barbon, A. P. A. C., & Barbin, D. F. (2019). Comparison of rapid techniques for classification of ground meat. *Biosystems Engineering, 183*, 151–159. https://doi.org/10.1016/j.biosystemseng.2019.04.013

Patel, N., Toledo-Alvarado, H., & Bittante, G. (2021). Performance of different portable and hand-held near-infrared spectrometers for predicting beef composition and quality characteristics in the abattoir without meat sampling. *Meat Science, 178*, Article 108518. https://doi.org/10.1016/j.meatsci.2021.108518

Rodriguez-Nogales, J. M. (2006). Approach to the quantification of milk mixtures by partial least-squares, principal component and multiple linear regression techniques. *Food Chemistry, 98*(4), 782–789. https://doi.org/10.1016/j.foodchem.2005.07.037

Wang, C., Wang, S., He, X., Wu, L., Li, Y., & Guo, J. (2020). Combination of spectra and texture data of hyperspectral imaging for prediction and visualization of palmitic acid and oleic acid contents in lamb meat. *Meat Science, 169*, Article 108194. https://doi.org/10.1016/j.meatsci.2020.108194

Wang, J., Xiao, J., Liu, X., Gao, Y., Luo, Z., Gu, X., & Geng, F. (2021). Tandem mass tag-labeled quantitative proteomic analysis of tenderloins between Tibetan and Yorkshire pigs. *Meat Science, 172*, Article 108343. https://doi.org/10.1016/j.meatsci.2020.108343

Xin, L., Zhang, Y. F., Duan, W. S., Ai, M. Y., Song, H. B., Huang, Q., & Lu, J. K. (2021). Effect of malondialdehyde oxidation on structure and physicochemical properties of amandin. International Journal of Food Science and Technology. doi: 10.1111/ijfs.15213.

Xiong, Z., Sun, D. W., Pu, H., Xie, A., Han, Z., & Luo, M. (2015). Non-destructive prediction of thiobarbituricacid reactive substances (TBARS) value for freshness evaluation of chicken meat using hyperspectral imaging. *Food Chemistry, 179*, 175–181. https://doi.org/10.1016/j.foodchem.2015.01.116

Yang, Q., Sun, D. W., & Cheng, W. (2017). Development of simplified models for nondestructive hyperspectral imaging monitoring of TVB-N contents in cured meat during drying process. *Journal of Food Engineering, 192*, 53–60. https://doi.org/10.1016/j.jfoodeng.2016.07.015

Yao, X., Cai, F., Zhu, P., Fang, H., Li, J., & He, S. (2019). Non-invasive and rapid pH monitoring for meat quality assessment using a low-cost portable hyperspectral scanner. *Meat Science, 152*, 73–80. https://doi.org/10.1016/j.meatsci.2019.02.017

Zhang, H., Ai, M., Shi, F., He, H., Song, H., Luo, Z., & Lu, J. (2020). Deterioration mechanism of minced mutton induced by Fenton oxidation treatment. *LWT - Food Science and Technology, 134*, Article 109980. https://doi.org/10.1016/j.lwt.2020.109980

Zhenjie, X., Dawen, S., Qiong, D, & Zeng, H. (2014). Application of visible hyperspectral imaging for prediction of springiness of fresh chicken meat. Food Analytical Methods, 8, 380-319, doi: 10.1007/s12161-014-9853-3.

Further reading

Brasil, Y. L., Cruz-Tirado, J. P., & Barbin, D. F. (2022). Fast online estimation of quail eggs freshness using portable NIR spectrometer and machine learning. *Food Control, 131*, Article 108418. https://doi.org/10.1016/j.foodcont.2021.108418